Published in final edited form as:
Immunity. 2010 December 14; 33(6): 853–862. doi:10.1016/j.immuni.2010.11.026.

The 2.5 Å structure of CD1c in complex with a mycobacterial lipid reveals an open groove ideally suited for diverse antigen presentation

Louise Scharf[1], **Nan-Sheng Li**[1], **Andrew J. Hawk**[2], **Diana Garzón**[3], **Tejia Zhang**[4], **Lisa M. Fox**[5], **Allison R. Kazen**[1], **Sneha Shah**[1], **Esmael J. Haddadian**[1], **Jenny E. Gumperz**[5], **Alan Saghatelian**[4], **José D. Faraldo-Gómez**[3,6], **Stephen C. Meredith**[1,2], **Joseph A. Piccirilli**[1,7], and **Erin J. Adams**[1,8]

[1] Department of Biochemistry and Molecular Biology, University of Chicago, Chicago, USA

[2] Department of Pathology, University of Chicago, Chicago, USA

[3] Theoretical Molecular Biophysics Group, Max Planck Institute of Biophysics, Frankfurt am Main, Germany

[4] Department of Chemistry and Chemical Biology, Harvard University, Cambridge, USA

[5] Department of Medical Microbiology and Immunology, University of Wisconsin School of Medicine and Public Health, Madison, Wisconsin, United States of America

[6] Cluster of Excellence 'Macromolecular Complexes', Goethe University Frankfurt, Frankfurt am Main, Germany

[7] Department of Chemistry, University of Chicago, Chicago, USA

[8] Committee on Immunology, University of Chicago, Chicago, USA

Summary

CD1 molecules function to present lipid-based antigens to T cells. Here we present the crystal structure of CD1c at 2.5 Å resolution, in complex with the pathogenic *Mycobacterium tuberculosis* antigen mannosyl-β1-phosphomycoketide (MPM). CD1c accommodated MPM's methylated alkyl chain exclusively in the A′ pocket, aided by a unique exit portal underneath the α1 helix. Most striking was an open F′ pocket architecture lacking the closed cavity structure of other CD1 molecules, reminiscent of peptide binding grooves of classical Major Histocompatibility Complex molecules. This feature, combined with tryptophan-fluorescence quenching during loading of a dodecameric lipopeptide antigen, provides a compelling model by which both the lipid and peptide moieties of the lipopeptide are involved in CD1c presentation of lipopeptides.

Contact: Erin J. Adams, Department of Biochemistry and Molecular Biology, University of Chicago. 929 E. 57th St. GCIS W236. Phone: 773-834-9816, ejadams@uchicago.edu.

Accession Numbers: Coordinates and structure factors for the complex of CD1c with MPM have been deposited in the Protein Data Bank under the accession code 3OV6.

Introduction

CD1 molecules are Major Histocompatibility Complex (MHC)-like proteins that are broadly expressed on antigen-presenting cells (APCs) and serve to present lipid-based antigens to T cells in the vertebrate immune response. Unlike the polymorphic, peptide-presenting, classical class I and II MHC molecules, CD1 proteins exhibit essentially no allelic variation, and in humans are located outside of the Chromosome 6 MHC region on Chromosome 1 at 1q22–23 (Albertson et al., 1988). There exist five human isoforms of CD1 that are grouped according to their amino acid homology, genomic organization and immunological function; CD1a, CD1b, and CD1c form Group 1 (Calabi et al., 1989), CD1d forms Group 2 and CD1e has been proposed to form a third group due to its intracellular chaperone function (Angenieux et al., 2000; de la Salle et al., 2005). Tyrosine-containing motifs present in the cytoplasmic tail of CD1b, CD1c and CD1d molecules determine where they are trafficked within the cell, and thus to what repertoire of lipid-based antigens they may be exposed. The trafficking route as well as structural features unique to each CD1 molecule endow them with the ability to bind a structurally diverse array of lipid antigens from bacterial (Willcox et al., 2007) and endogenous sources (De Libero and Mori, 2007) and present these to T cells at the cell surface (Sullivan and Kronenberg, 2007).

CD1 molecules have evolved a deep and narrow binding cavity that is well suited to anchoring the hydrophobic alkyl chains of lipid molecules. Based on the structures of CD1a (Zajonc et al., 2005b; Zajonc et al., 2003), CD1b (Batuwangala et al., 2004; Gadola et al., 2002) and mouse (Wu et al., 2006; Zajonc et al., 2005a; Zajonc et al., 2005c; Zajonc et al., 2008; Zeng et al., 1997) and human CD1d (Koch et al., 2005), the binding cavity contains two major pockets, A′ and F′. In each of these structures the A′ pocket extends deep into the CD1 molecule and is enclosed by the A′ roof. Variation in the A′ pocket size, the shape of the F′ pocket along with the presence of an exit portal (C′) and T′ tunnel unique to CD1b explain each isoform's ability to bind different classes of lipids, varying in the length and saturation of their hydrocarbon tails and the chemical nature of their head group.

Of the CD1 isoforms, CD1c is unique in its ability to present mycobacterial phosphoketides (de Jong et al., 2007; Matsunaga et al., 2004) and polyisoprenoids (Moody et al., 2000) containing branched alkyl chains and has also been shown to present lipopeptides with a long peptide moiety similar in length to those presented by MHC class II molecules (Moody et al., 2004; Van Rhijn et al., 2009). CD1c is expressed at high amounts on B cells, myeloid dendritic cells (DCs) and thymocytes (Dougan et al., 2007) and intracellularly it broadly surveys the endocytic system (Sugita et al., 2000), particularly early and late endosomes (Briken et al., 2002; Briken et al., 2000) similar to the path of MHC class II proteins. CD1c is the only CD1 isoform that has been shown to interact with both αβ (Beckman et al., 1996; Porcelli et al., 1989; Van Rhijn et al., 2009) and γδ (Spada et al., 2000) T cells to date.

Functionally, CD1c has a clear role in mediating T cell responses to infectious pathogens, in particular *Mycobacterium tuberculosis*, the causative agent of tuberculosis (Beckman et al., 1996; Moody et al., 2000; Ulrichs et al., 2003). This was further elucidated through elegant studies of CD1c presentation of synthetic forms of mannosyl phosphodolichols (MPDs) and mannosyl-β1-phosphomycoketides (MPMs) identical to those present in minute quantities in the cell walls of *M. tuberculosis* and *M. avium* (de Jong et al., 2007; Moody et al., 2000). T cell-specific, CD1c-presented MPMs contain structurally distinct single alkyl chains ranging from $C_{30–34}$ that have stereo-specific (S) methyl branches starting at C_4, repeated on every fourth carbon thereafter (de Jong et al., 2007). Made by polyketide synthase 12 (pks12) (Matsunaga et al., 2004), an enzyme that appears to be unique to mycobacteria, the methyl branches of MPM represent an unusual pathogen-associated molecular pattern that, when presented at even minute amounts by CD1c, can potently activate a T cell response.

The molecular features of CD1c that enable it to bind and present the structurally divergent MPM and 12-mer lipopeptide antigens have remained unclear. Computational modeling and molecular dynamics simulations have provided hints of divergent features of CD1c (Garzon et al., 2009); however an experimentally derived three-dimensional structure has evaded determination. Our 2.5 Å crystal structure of CD1c in complex with a synthetic, all-S, C_{32} mannosyl-β1-phosphomycoketide (MPM) demonstrates how CD1c accommodates the unique methyl-branched structure of mycoketides, and reveals an open F′ groove feature that may explain CD1c's ability to bind and present dodecameric lipopeptides (lipo-12).

Results

Crystallization and structure determination of CD1c in complex with MPM

Recombinant expression of CD1c was performed using the baculovirus insect expression system. An initial, expression-optimized construct was designed by fusing the $\beta_2$microglobulin (β_2m) subunit covalently to the N-terminus of CD1c via a 15 amino acid glycine-serine linker. Repeated attempts to crystallize this construct failed, so a crystal contact-optimized construct was further generated by swapping the CD1c α3 domain for that of the α3 domain of CD1b. Additional mutations were made to stabilize the interface between the platform and α3 domain, reduce the heterogeneity of glycosylation (four of the five putative N-linked glycosylation sites were eliminated), and to facilitate crystal packing (see Supplementary Methods). Several methods were used to establish that the CD1c α1 and α2 platform domain in this optimized mutant was functionally and structurally conserved in relation to wild-type CD1c. CD spectra of wild-type and optimized CD1c were super-imposable (Figure 1A) demonstrating overall secondary structure similarity between the two proteins. Furthermore, size-exclusion chromatography and native polyacrylamide gel shift demonstrated similar binding of the CD1c-specific F10/21A3 and L161 antibodies to both wild-type and optimized CD1c (Figures 1B and 1C), confirming that the three-dimensional epitopes of these antibodies on these two CD1c constructs was conserved. To assess the functional conservation of our optimized CD1c construct, we performed lipid loading assays based on isoelectric focusing (IEF) gel-shift similar to those described by Zhou *et al.* (Zhou et al., 2004) and confirmed that lipid binding was not compromised by the modifications made to CD1c to facilitate crystallization (Figure 1D). Furthermore, optimized CD1c loaded with our synthetic MPM was able to stimulate the CD8-1 T cell line, which is specific for CD1c presenting MPM, at equivalent amounts to that of native CD1c presenting MPM (Figure 1E), confirming the functional conservation of these two constructs.

Chemically synthesized mannosyl-β1-phosphomycoketide (MPM) was passively loaded into recombinant, optimized, CD1c and the resulting complex was purified by gel filtration chromatography. The complex of CD1c and MPM was crystallized and the structure was determined using molecular replacement with CD1b as the initial model. There was one complex of CD1c and MPM in the asymmetric unit. The structure was refined to 2.5 Å with a final R_{cryst} and R_{free} of 24.0% and 27.3%, respectively, and 93.3% of the residues in the most favored region of the Ramachandran plot. (Figure 2 and Table 1). A loop connecting the α1 helix to the β-sheet was poorly resolved in the electron density and residues Q87–Y89 were excluded from the final model as a result. Furthermore, only the first four amino acids of the glycine and serine linker engineered to fuse β_2m and the CD1c heavy chain were resolved in the electron density. Amino acid side chains with weak or absent electron density had their occupancies set to zero.

Examination of crystallographic symmetry mates revealed that the K108G mutation engineered into the $CD1c_{opt}$ construct was critical to the establishment of a key crystal contact with a loop (residues 261 to 276) in the α3 domain of a symmetry mate. The

presence of a large charged side chain at position 108 would create a steric clash and disrupt a crystal contact at this location.

Structural topology of the CD1c binding groove: Conserved features

The CD1c heavy chain is composed of α1, α2 and α3 domains that assemble non-covalently with the β_2m subunit, similar to other CD1 family members. The α1 and α2 domains constituted the ligand-binding platform domain and have the canonical MHC structure of two α-helices supported by a six-stranded β-sheet (Figure 2A, 2B). This architecture supported the formation of two distinct ligand-binding cavities, lined with hydrophobic residues that are compatible with the binding of hydrophobic alkyl chains characteristic of lipid molecules. These two cavities have been named A′ and F′ based on homology with the peptide-binding pockets of MHC class I molecules and consistent with the pocket nomenclature for other CD1 family members (Zeng et al., 1997). The platform domain (α1 and α2 domains) of CD1c was most structurally related to that of CD1b based on a backbone RMSD of 1.16 Å (in comparison to CD1a: 1.50 A and CD1d: 1.60 A) consistent with CD1c's close (59%) amino acid identity to CD1b (Figure S1).

CD1c's A′ pocket had the shape of a wide circular tunnel with one area of constriction, located slightly underneath the A′ portal, where the A′ pocket opened to solvent (Figure 3, top panel). This constriction selected for a clockwise directionality for lipid binding in the A′ pocket, specifically for those lipids with methylated branches, as seen in MPM. CD1c's circular A′ pocket was centered around the A′ pole formed by the van der Waals contact of V12 and F70. The A′ pole as well as the A′ roof, composed of residues L66, L162 and T166, made up the conserved features of the A′ pocket found in other CD1 isoforms (Figure 3). The A′ portal is rimmed with the hydrophobic residues L69, F72, Y73 and V155, and the polar T158; it is here where the phosphomannose head group of MPM was situated, in a conformation consistent with presentation to a T cell receptor (TCR) (Figure 2). The A′ portal was continuous with the F′ pocket, lacking a dividing wall between these two cavities (Figure 2A, lower panel). In comparison to the other human CD1 isoforms, CD1c had the second largest cavity volume, 1780 $Å^3$, compared with CD1b (2200 $Å^3$), CD1d (1650 $Å^3$) and CD1a (1280 $Å^3$) as calculated by the program Pocket-Finder (Hendlich et al., 1997). Therefore the overall structure of CD1c in complex with MPM was reminiscent of other CD1 isoforms in the location and chemical nature of their A′ and F′ pockets.

Structural topology of the CD1c binding groove: Unique features

Unique to CD1c was the presence of a portal to the exterior located underneath the α1 helix, called the D′ portal due to its similarity in location to the D pocket in MHC class I molecules. Two amino acid substitutions only found in CD1c (G26 and L74) are involved in the architecture of this portal, with contributions from G28 (found in other CD1 isoforms) (Figure 4A, upper panel, Figure S1). In CD1b, most closely related to CD1c based on structural and amino acid homology, T26 and I74 closed off this portal to the exterior, despite sharing the glycine at position 28 (Figure 4A, lower panel, Figure S1). An additional opening was noted in the CD1c structure, called the E′ portal, which connects the F′ pocket to the exterior through a narrow tunnel under the α1 helix. This opening was formed by several amino acids that are either unique to CD1c (F16, L77 and V96) or are shared with other isoforms (F18, T78, I81) (Figure 4A, upper panel, Figure S1). Key to the formation of both portals was the increased distance between the α1 helix and the S2 β-strand of the α1 domain β-sheet, due in part to the presence of the large aromatic side chain at position 16 (F16) (Figure 4B, Figure S1). This caused a ~2.5 Å increase in main chain-main chain distance between the α1 helix and β-sheet at the location of these portals (Figure 4B).

The most striking aspect of CD1c was the open nature of the F′ pocket, here termed the F′ groove, a feature not found in other CD1 molecules (Figure 5). CD1c's F′ groove is open to solvent, contrasting with the closed nature of the F′ pockets of other CD1 isoforms. This open groove was created by both smaller side chains in CD1c at positions 84, 140 and 144 (H, L and V in contrast to F, R and F in CD1b) which failed to reach across the α1 and α2 helical divide, and the extended conformation of the connecting loop between the α1 helix and the S1 strand of the α2 domain β-sheet (Figure 5, Figure S1). In all other CD1 molecules this loop is tucked back into the architecture of the F′ pocket, closing off this region to solvent (Figure 5, Figure S1). The residues lining the F′ groove in CD1c were almost entirely hydrophobic in nature; of the 21 side chain residues contributing to this surface only H84 is potentially charged (this side chain was also disordered in the electron density) whereas the remainder were composed of eight aromatic and twelve nonpolar residues (V, L or I). Therefore, ligands bound in this groove would preferentially be hydrophobic and/or aromatic in nature. It was also notable that the atomic displacement factors (or B-factors) were highest in the α-helical regions of the F′ groove (Figure S2), suggestive of a higher intrinsic disorder or flexibility to this region. This putative flexibility may be a contributing factor to CD1c's ability to accommodate alternative ligands in this groove, such as the lipopeptide ligands containing larger peptide fragments.

Mannosyl-β1-phosphomycoketide presentation by CD1c

Liquid chromatography-mass spectrometry (LC-MS) of our CD1c loaded with MPM showed a significant enrichment of MPM, confirming that MPM was bound in our purified complex (Figure S3). The LC-MS analysis also revealed bound hydrocarbon chains ranging in length from C_8 to C_{18} (Figure S3). Omit map electron density showed a clear clockwise traverse of the methylated hydrocarbon chain of MPM through the A′pocket, exiting through the D′ portal (Figure 2 and Figure 4A). The C_{32} MPM (equivalent to the natural *M. tuberculosis* MPM) lipid tail was accommodated perfectly in the A′ pocket, demonstrating the optimal length of hydrocarbon chains for CD1c is approximately 27 carbons (the remaining five are methyl groups). The exact placement of the phosphomannose head group was unclear in initial rounds of refinement, so we used molecular dynamics simulations and energy minimization based on omit map density to estimate the optimal positioning of the MPM lipid ligand within the A′ pocket. Two positions were determined to be most likely based on these simulations, one designated A1 features optimal hydration and placement of the negatively charged phosphate group; the second, designated A2, was positioned according to electron density that extends out of the D′ portal, positioning the head group lower in the A′ portal in a less optimal hydrophobic environment (Figure S4). Further rounds of refinement with the lipid in the A1 position revealed omit map density for two water molecules consistent with a water-mediated stabilization of the head group (Figure 6). Five highly probable hydrogen bonds (distance < 3.3 Å, Table S1) coordinating the phosphomannose head group were evident and shown in Figure 6 as large dashes, four of which are water mediated. The fifth hydrogen bond was between the main chain carbonyl of F72 and the ring oxygen of the mannose. Additional potential hydrogen bonds were present (Figure 6 and Table S1, some, but not all, of these weak hydrogen bonds are indicated as small dashes) indicating that positioning of the phosphomannose head group in A1 was optimal both in regards to our electron density data and molecular dynamics simulations.

Density in the F′ groove of our CD1c structure was consistent with a C_{12} hydrocarbon chain, supported by our LC-MS analysis of lipids bound to CD1c. This LC-MS data showed that CD1c could also bind free fatty acids (FFAs) ranging from C_8 to C_{18}, with enrichment in C_{12} (Figure S3B). However, the presence of other hydrocarbon chains from these FFAs made it unclear whether the density in the structure represented a C_{12} hydrocarbon chain, an average of a population of variable hydrocarbon chain lengths (similar to the averaged

density present in the first "unloaded" CD1 structure of murine CD1d (Zeng et al., 1997)), and/or an alternatively placed MPM. Therefore we have conservatively placed a C_{12} hydrocarbon chain in the density to represent these possibilities. Molecular dynamics simulations suggested that a portion of MPM lipid tail could be stably bound in the F′ groove (Figure S4). However, the lack of sufficient electron density for the MPM lipid tail in the F′ groove suggested the most stable conformation for MPM is in the A′ pocket, as observed (Figures 2 and 3).

Presentation of lipopeptide antigens by CD1c

The unique F′ groove structure led us to speculate that this feature may allow CD1c to bind diverse antigens for presentation to T cells. Since previous work has demonstrated a clear role for CD1c in lipopeptide presentation through characterization of a stimulatory 12-mer lipopeptide similar in sequence to the myristoylated NEF (Van Rhijn et al., 2009), we sought to test whether the F′ groove played a role in binding of the peptide portion of this antigen. The defined sequence of the peptide motif: GGKWSKXSKWSK with acylation at the N-terminal glycine, contained two tryptophan residues and a kynurenine (designated as X), an oxidized form of tryptophan. Titration of this synthetic lipopeptide into a solution containing CD1c resulted in clear quenching of tryptophan fluorescence (Figure 7). Based on these titration data, the equilibrium binding constant (K_D) of this lipopeptide for CD1c was calculated to be ~66 nM. We therefore propose a model whereby the peptide moiety is associated with the F′ groove (either buried or associated with its surface) of CD1c while the acyl chain is accommodated in the A′ pocket, similar to what we observe for MPM.

Discussion

CD1 molecules, while non-polymorphic, have evolved specific structural features enabling them to bind and present unique repertoires of lipid-based ligands to T cells. All structural information to date suggests a model whereby CD1 molecules anchor their antigens through binding of their alkyl chains in pockets or tunnels, positioning the polar lipid head groups in their A′ or F′ portals, accessible to recognition by a T cell receptor. The size and complexity of these pockets dictates the lipid-based antigens that can be bound by each isoform. CD1a possesses a "molecular ruler" in the form of a restricted sized A′ pocket, limiting bound alkyl chains to a particular length. The F′ pocket of CD1a, however, can accommodate both the N-aryl branch of a siderophore lipopeptide (Zajonc et al., 2005b) or the fatty acid chain of a sulfatide (Zajonc et al., 2003). On the other hand, CD1b has evolved a connected network of A′, F′, C′ and T′ channels (Gadola et al., 2002), creating a "maze" that has the capacity to fit alkyl chains up to C_{80} in length. A unique C′ portal also allows variation in size of the bound lipid moiety, acting as an escape hatch for lipids of varying length. Mouse and human CD1d appear well suited to bind diacylated lipids (Koch et al., 2005; Wu et al., 2006; Zajonc et al., 2005a; Zajonc et al., 2005c; Zajonc et al., 2008; Zeng et al., 1997) such as the canonical α-galactosylceramide (α-GalCer), a potent agonist for the CD1d-restricted invariant Natural Killer T cell population. The acyl chain of CD1d-bound lipids is bound in the A′ pocket whereas the sphingosine or phytosphingosine chains are found in the F′ pocket. We have shown here that CD1c, the last of the lipid-presenting human isoforms to be structurally characterized, has structural features unlike those present in the other human CD1 isoforms. These features endow CD1c with the unique ability to present divergent antigens such as the branched mycoketide, MPM, from *M. tuberculosis* and lipopeptides with long peptide moieties.

In our structure, MPM appears bound exclusively in the A′ pocket, exiting through the D′ portal underneath the α1 helix. It is this portal, unique to CD1c, that appears to allow the preferential binding of the branched alkyl chain of MPM, and enables the observed variation in length (C_{30}–C_{34}) of MPM that can activate T cells when presented in CD1c (de Jong et

al., 2007). Similar to other complexes of CD1 molecules with lipids, this binding mode situates the polar phosphomannose head group ideally for recognition by a T cell receptor. The electron density of MPM in our structure was consistent with two alternative conformations; molecular dynamics simulations with energy minimization favored the A1 conformation consistent with optimal solvation and hydrogen bonding of the phosphomannose head group. However, the electron density for the alkyl chain extended out the D′ portal, suggesting that the computationally less preferred A2 conformation may also exist in our structure.

Our structure also provides a rationale for CD1c's specificity for MPM's lipid length and stereochemistry of methylation. Longer length mannosyl-β2-phosphodolichol (MPD) analogs of the length $C_{55–95}$ are essentially non-stimulatory to CD1c-reactive T cells (Moody et al., 2000); alkyl chains of this length would have to extend either out of the D′ portal or out of the A′ portal into solvent, both highly energetically unfavorable conformations and therefore not preferred for binding into CD1c. Furthermore, due to the constriction in the circular A′ pocket, it is unlikely that longer branched alkyl chains could wrap around this pocket in the fashion seen in CD1b (Gadola et al., 2002). Our structure also reveals why the natural, all-S conformation of *M. tuberculosis* C_{32} MPM is preferred over synthetic, stereorandom C_{30} MPM which produces a 20 to 40-fold decrease in stimulation of the CD8–1 T cell clone which recognizes the complex of CD1c with MPM (de Jong et al., 2007). Based on the turn that is present in the all-S C_{32} MPM in our structure, alternative positioning of the last four methyl groups of MPM would force them to point inward in the turn, clashing with the natural turn of the A′ pocket. The all-S form has these last four methyl groups splayed to the outside of the turn, allowing for a tighter bend to the alkyl chain. Because $1/16^{th}$ (2^{-4}) of the stereorandom MPM mixture would be composed of all-S methyl groups in these positions, this would explain the decrease, yet not abolition, of the T cell stimulation activity of this mixture.

We and others have shown that CD1c can also bind diacylated lipids similar to those found in other CD1 isoforms (Gilleron et al., 2004; Guiard et al., 2009; Shamshiev et al., 2002), so it is likely that CD1c can stably bind two alkyl chains in its A′ and F′ pockets. However, accommodation of a single alkyl chain such as that seen in MPM likely requires the presence of the methyl branches to stabilize it in the CD1c A′ pocket. Removal of these methyl branches results in a drastic decrease in T cell simulation (de Jong et al., 2007), likely due to the weakened stability of these MPM variants in CD1c. The electron density apparent in the F′ groove of CD1c suggests that this structure, while open to solvent, maintains the ability to bind alkyl chains. Indeed, a variety of free fatty acids, enriched in the hydrocarbon chain C_{12}, were characterized by LC-MS from our MPM loaded CD1c. Furthermore, molecular dynamics simulations suggest that MPM can also be bound in the F′ groove, although our structure suggests that it is not accommodated with the same occupancy or stability as that seen in the A′ pocket. Thus, the electron density we see is likely due to averaging over the various lipid species that may be bound in the F′ groove.

The presence of the F′ groove provides a compelling explanation for how CD1c can bind, at high affinity, divergent ligands such as the dodecameric lipopeptide (lipo-12) that mimics myristoylated proteins (Van Rhijn et al., 2009). Myristoylation is the process by which myristate (saturated C_{14}) is covalently attached via an acyl linkage to an N-terminal glycine residue. Vital to eukaryotic cellular processes and required for the functioning of certain viral proteins (such as the myristoylated Nef (Guy et al., 1987) and Gag (Veronese et al., 1988) proteins of the Human Immunodeficiency Virus (HIV), myristolation is predicted to occur on ~0.8% of mammalian proteins and ~3.7% of viral proteins (http://mendel.imp.ac.at/myristate/myrbase/). The affinity calculated for lipo-12 (~66 nM) is similar in magnitude to that of lipoarabinomannan (LAM) for CD1b (32 nM-53 nM) (Ernst

et al., 1998) and to those measured for high-affinity peptides for MHC molecules. Both are higher than the measured affinities for CD1d and αGalCer (ranging from 340 nM (Naidenko et al., 1999) to ~1–10 μM (Cantu et al., 2003)). It is important to note that in all cases, these are relative measurements as CD1 molecules are likely loaded with endogenous lipids during eukaryotic synthesis or detergent molecules during refolding. In addition, lipids most likely exist in a micellar form depending on their critical micellar concentration (CMC). Thus these measurements reflect a combination of parameters, including removal of lipids from the micellar state and competition with CD1-bound lipid. However, our affinity measurements for lipo-12 and CD1c suggest involvement of the peptidic portion of the antigen, considering that unbranched, saturated synthetic versions of MPM are not stimulatory and therefore unlikely to be stably bound (de Jong et al., 2007).

Supported by our tryptophan fluorescence quenching results and affinity determination, we propose a model where the acyl chain of lipo-12 is bound in the A′ pocket, similar to the branched alkyl chain of MPM, while the peptide portion, anchored by the two tryptophans and one kynurenine, is bound in the F′ groove. It is important to note, however, that tryptophan fluorescence quenching can be caused by a variety of factors including small structural changes in the protein and therefore does not provide direct evidence of the peptide portion being bound in the F′ groove. In the absence of a crystal structure of the complex of CD1c and lipo12, other models are also plausible, such as the peptide portion associating with the surface of CD1c, outside of the F′ groove. Shorter lipopeptides, or alteration of the amino acid sequence of the peptide portion, can affect T cell reactivity (Van Rhijn et al., 2009), however it awaits further analysis to determine whether alteration of these residues affects lipopeptide loading and stability in CD1c. This model of lipopeptide presentation by CD1c provides insight into how acylated proteins can be recognized as pathogenic patterns, raising questions about how CD1c-reactive T cells may discriminate between endogenous and foreign lipopeptides.

Experimental Procedures

Synthesis of Mannosyl-β1-phosphomycoketide

The synthesis of mannosyl-β1-phosphomycoketide (or*β*-D-mannosyl phosphomycoketide) (MPM) (structure #**29**) is outlined in Supplementary Methods: Schemes S1-S5. Starting from commercially available methyl (2*S*)-3-hydroxy-2-methylpropionate (**1**), compounds **11** (Scheme S1), **17** (Scheme S2) and **22** (Scheme S3) were prepared. Using a sequence of reactions that included Julia-Kocienski coupling, platinum- and palladium-catalyzed hydrogenations and the Dess-Martin oxidation, these fragments were connected synthetically (Scheme S4) in good yield to give the precursor mycoketide C7 (*n*-heptyl at the tail end of the lipid). The synthesized mycoketide was used to prepare mannosyl-β1-phosphomycoketide **29** according to a literature procedure (Scheme S5) (Summeren et al., 2006). The mass spectrum and other analytical data confirmed the structure of **29**. Negative ion MS Calcd for $C_{38}H_{79}O_9P^-$ ($M\text{-}Na^+$): 707.5, found: 707.4. Synthetic details will be reported elsewhere.

Protein expression, purification and crystallization

The $CD1c_{opt}$ construct was subcloned into the baculovirus transfer vector pAcGP67A (BD Biosciences) with a deca-His tag and expressed in High Five cells using the baculovirus expression system (Saphire Baculovirus DNA-Orbigen). The protein was purified with Ni-NTA resin, eluted with buffer containing 200 mM imidazole, and treated with carboxypeptidase A (Sigma) at 25°C overnight to remove the C-terminal His-tag. The protein was further purified by gel filtration using a Superdex 200 column (GE Healthcare)

equilibrated with Hepes Buffered Saline (HBS: 10mM Hepes, pH 7.2, 150mM NaCl, 0.02% azide).

To load MPM into CD1c, 0.2 mg of MPM per 1 mg of CD1c were incubated at 37°C for 30 min in HBS containing 0.05% Tween 20. The CD1c-MPM complex was repurified by gel filtration using a Superdex 200 column equilibrated in HBS containing 50mM NaCl to remove excess lipid and detergent. For crystallization, peak fractions were pooled and concentrated to 10 mg/mL. Crystallization screens were carried out using the sitting drop method and initial hits were optimized in both sitting and hanging drops by varying pH, precipitant concentration and the use of additives. The best crystals were obtained using a hanging-drop setup at 18°C by combining 1 μL protein solution and 1 μL mother liquor containing 1.05 M sodium citrate, 100 mM CHES pH 9.4 and 25 mM triglycine.

Data collection and processing

X-ray data sets were measured on a MAR300 CCD at beamline 23 ID-D at the Advanced Photon Source (APS) at Argonne National Laboratory. Crystals were cryoprotected with 50% sodium malonate before cooling to 100°K. A complete 2.5 Å data set was collected using 1° oscillations over 150 frames and a 1.033×10^{-10} m wavelength. The crystals indexed in space group $P2_12_12_1$ with unit cell dimensions a=53.72 Å, b=87.09 Å, c=88.81 Å. HKL2000 was used to index, integrate and scale the data (Otwinowski and Minor, 1997). Data statistics are shown in Table 1.

Structure determination and analysis

Using a CD1b heavy chain and β_2m (Garcia-Alles L.F., 2006) as a search model, stepwise molecular replacement with Phaser (A. J. McCoy, 2007) located the single CD1c molecule per asymmetric unit. Rigid body refinement was performed using Phenix (P. D. Adams, 2010), followed by manual building using Coot (Emsley and Cowtan, 2004) and individual site and B-factor refinement using Phenix (P. D. Adams, 2010). The stereochemistry of the model was improved using a backbone optimization procedure incorporating a torsional statistical potential contingent on amino acid type, its secondary structure as well as the identity of its two neighbors (DeBartolo et al., 2009), followed by real space refinement using a two step algorithm developed by E.J. Haddadian, K.F. Freed and T.R.Sosnick (manuscript in preparation). Both composite (Phenix (P. D. Adams, 2010)) and simple (CCP4 Sfcheck (C.C.P.4., 1994)) omit maps were calculated at each stage to locate density for ligands that were not present in the model. Hydrogen bonding contacts between MPM and CD1c were calculated using the program Contacts (CCP4 program package (C.C.P.4., 1994)). Main-chain RMSD values between CD1c and CD1a, CD1b and CD1d were calculated using PDBeFold (Krissinel and Henrick). Total ligand binding groove volumes of CD1a, CD1b, CD1c and CD1d were computed using Pocket-Finder (an algorithm based on Ligsite (Hendlich et al., 1997)). All structural figures were generated using the program Pymol (DeLano Scientific).

Analysis of lipopeptide binding with fluorescence spectroscopy

To measure binding of lipo-12 to CD1c, 1 mL samples containing 10 nM CD1c in HBS and various concentrations of lipo-12 ranging from 5 nM-10 μM were incubated at 37°C for 1 hour. Tryptophan fluorescence of the sample was measured using a PTI fluorimeter (model 810) with an excitation wavelength of 280 nm and the maximum emission signal at 340 nm was observed. The quenching of tryptophan fluorescence with increasing amounts of lipo-12 was expressed as a ratio $(E-E_o)/E_o$, the change in fluorescence divided by the control fluorescence in the absence of added lipo-12. The signal ratio was plotted against lipo-12 concentration and fit using non-linear regression in GraphPad Prism to a one-site binding model.

Supplementary Material

Refer to Web version on PubMed Central for supplementary material.

Acknowledgments

We thank the staff of the Advanced Proton Source at GM/CA-CAT (23ID) and LS-CAT (21ID) for their use and assistance with X-ray beamlines; Ruslan Sanishvili and Joseph Brunzelle in particular for help and advice during data collection; Esmael Haddadian, Karl F. Freed and Tobin R. Sosnick for use of their torsion angle plus real space refinement algorithm; Michael Brenner for the CD1c cDNA and Albert Bendelac for helpful discussions. This study was supported by National Institutes of Health grants R01AI073922 and R01GM081642 and the Kinship Foundation Searle Scholars Award to Erin J. Adams.

References

McCoy AJ, RWGK, Adams PD, Winn MD, Storoni LC, Read RJ. Phaser crystallographic software. J Appl Cryst. 2007; 40:658–674. [PubMed: 19461840]

Albertson DG, Fishpool R, Sherrington P, Nacheva E, Milstein C. Sensitive and high resolution in situ hybridization to human chromosomes using biotin labelled probes: assignment of the human thymocyte CD1 antigen genes to chromosome 1. EMBO J. 1988; 7:2801–2805. [PubMed: 3053166]

Angenieux C, Salamero J, Fricker D, Cazenave JP, Goud B, Hanau D, de La Salle H. Characterization of CD1e, a third type of CD1 molecule expressed in dendritic cells. J Biol Chem. 2000; 275:37757–37764. [PubMed: 10948205]

Batuwangala T, Shepherd D, Gadola SD, Gibson KJ, Zaccai NR, Fersht AR, Besra GS, Cerundolo V, Jones EY. The crystal structure of human CD1b with a bound bacterial glycolipid. J Immunol. 2004; 172:2382–2388. [PubMed: 14764708]

Beckman EM, Melian A, Behar SM, Sieling PA, Chatterjee D, Furlong ST, Matsumoto R, Rosat JP, Modlin RL, Porcelli SA. CD1c restricts responses of mycobacteria-specific T cells. Evidence for antigen presentation by a second member of the human CD1 family. J Immunol. 1996; 157:2795–2803. [PubMed: 8816382]

Briken V, Jackman RM, Dasgupta S, Hoening S, Porcelli SA. Intracellular trafficking pathway of newly synthesized CD1b molecules. EMBO J. 2002; 21:825–834. [PubMed: 11847129]

Briken V, Jackman RM, Watts GF, Rogers RA, Porcelli SA. Human CD1b and CD1c isoforms survey different intracellular compartments for the presentation of microbial lipid antigens. J Exp Med. 2000; 192:281–288. [PubMed: 10899914]

CCP4. The CCP4 Suite: Programs for Protein Crystallography. Acta Cryst D. 1994; 50:760–763. [PubMed: 15299374]

Calabi F, Jarvis JM, Martin L, Milstein C. Two classes of CD1 genes. Eur J Immunol. 1989; 19:285–292. [PubMed: 2467814]

Cantu C 3rd, Benlagha K, Savage PB, Bendelac A, Teyton L. The paradox of immune molecular recognition of alpha-galactosylceramide: low affinity, low specificity for CD1d, high affinity for alpha beta TCRs. J Immunol. 2003; 170:4673–4682. [PubMed: 12707346]

de Jong A, Arce EC, Cheng TY, van Summeren RP, Feringa BL, Dudkin V, Crich D, Matsunaga I, Minnaard AJ, Moody DB. CD1c presentation of synthetic glycolipid antigens with foreign alkyl branching motifs. Chem Biol. 2007; 14:1232–1242. [PubMed: 18022562]

de la Salle H, Mariotti S, Angenieux C, Gilleron M, Garcia-Alles LF, Malm D, Berg T, Paoletti S, Maitre B, Mourey L, et al. Assistance of microbial glycolipid antigen processing by CD1e. Science. 2005; 310:1321–1324. [PubMed: 16311334]

De Libero G, Mori L. Structure and biology of self lipid antigens. Curr Top Microbiol Immunol. 2007; 314:51–72. [PubMed: 17593657]

DeBartolo J, Colubri A, Jha AK, Fitzgerald JE, Freed KF, Sosnick TR. Mimicking the folding pathway to improve homology-free protein structure prediction. Proc Natl Acad Sci U S A. 2009; 106:3734–3739. [PubMed: 19237560]

Dougan SK, Kaser A, Blumberg RS. CD1 expression on antigen-presenting cells. Curr Top Microbiol Immunol. 2007; 314:113–141. [PubMed: 17593659]

Emsley P, Cowtan K. Acta Cryst D. 2004; 60:2126–2132. [PubMed: 15572765]

Ernst WA, Maher J, Cho S, Niazi KR, Chatterjee D, Moody DB, Besra GS, Watanabe Y, Jensen PE, Porcelli SA, et al. Molecular interaction of CD1b with lipoglycan antigens. Immunity. 1998; 8:331–340. [PubMed: 9529150]

Gadola SD, Zaccai NR, Harlos K, Shepherd D, Castro-Palomino JC, Ritter G, Schmidt RR, Jones EY, Cerundolo V. Structure of human CD1b with bound ligands at 2.3 A, a maze for alkyl chains. Nat Immunol. 2002; 3:721–726. [PubMed: 12118248]

Garcia-Alles LF, VK, Maveyraud L, Vallina AT, Sansano S, Bello NF, Gober HJ, Guillet V, de la Salle H, Puzo G, Mori L, Heck AJ, De Libero G, Mourey L. Endogenous phosphatidylcholine and a long spacer ligand stabilize the lipid-binding groove of CD1b. EMBO J. 2006; 25:3684–3692. [PubMed: 16874306]

Garzon D, Bond PJ, Faraldo-Gomez JD. Predicted structural basis for CD1c presentation of mycobacterial branched polyketides and long lipopeptide antigens. Mol Immunol. 2009; 47:253–260. [PubMed: 19828201]

Gilleron M, Stenger S, Mazorra Z, Wittke F, Mariotti S, Bohmer G, Prandi J, Mori L, Puzo G, De Libero G. Diacylated sulfoglycolipids are novel mycobacterial antigens stimulating CD1-restricted T cells during infection with Mycobacterium tuberculosis. J Exp Med. 2004; 199:649–659. [PubMed: 14981115]

Guiard J, Collmann A, Garcia-Alles LF, Mourey L, Brando T, Mori L, Gilleron M, Prandi J, De Libero G, Puzo G. Fatty acyl structures of mycobacterium tuberculosis sulfoglycolipid govern T cell response. J Immunol. 2009; 182:7030–7037. [PubMed: 19454700]

Guy B, Kieny MP, Riviere Y, Le Peuch C, Dott K, Girard M, Montagnier L, Lecocq JP. HIV F/3′ orf encodes a phosphorylated GTP-binding protein resembling an oncogene product. Nature. 1987; 330:266–269. [PubMed: 3118220]

Hendlich M, Rippmann F, Barnickel G. LIGSITE: automatic and efficient detection of potential small molecule-binding sites in proteins. J Mol Graph Model. 1997; 15:359–363. [PubMed: 9704298]

Koch M, Stronge VS, Shepherd D, Gadola SD, Mathew B, Ritter G, Fersht AR, Besra GS, Schmidt RR, Jones EY, et al. The crystal structure of human CD1d with and without alpha-galactosylceramide. Nat Immunol. 2005; 6:819–826. [PubMed: 16007090]

Krissinel, E.; Henrick, K. Protein structure comparison service SSM. European Bioinformatics Institute;

Matsunaga I, Bhatt A, Young DC, Cheng TY, Eyles SJ, Besra GS, Briken V, Porcelli SA, Costello CE, Jacobs WR Jr, et al. Mycobacterium tuberculosis pks12 produces a novel polyketide presented by CD1c to T cells. J Exp Med. 2004; 200:1559–1569. [PubMed: 15611286]

Moody DB, Ulrichs T, Muhlecker W, Young DC, Gurcha SS, Grant E, Rosat JP, Brenner MB, Costello CE, Besra GS, et al. CD1c-mediated T-cell recognition of isoprenoid glycolipids in Mycobacterium tuberculosis infection. Nature. 2000; 404:884–888. [PubMed: 10786796]

Moody DB, Young DC, Cheng TY, Rosat JP, Roura-Mir C, O'Connor PB, Zajonc DM, Walz A, Miller MJ, Levery SB, et al. T cell activation by lipopeptide antigens. Science. 2004; 303:527–531. [PubMed: 14739458]

Naidenko OV, Maher JK, Ernst WA, Sakai T, Modlin RL, Kronenberg M. Binding and antigen presentation of ceramide-containing glycolipids by soluble mouse and human CD1d molecules. J Exp Med. 1999; 190:1069–1080. [PubMed: 10523605]

Otwinowski Z, Minor W. Methods Enzymol. 1997; 276:307–326.

Adams PD, PVA, Bunkóczi G, Chen VB, Davis IW, Echools N, Headd JJ, Hung L-W, Kapral GJ, Grosse-Kunstleve RW, McCoy AJ, Moriarty NW, Oeffner R, Read RJ, Richardson DC, Richardson JS, Terwilliger TC, Zwart PH. PHENIX: a comprehensive Python-based system for macromolecular structure solution. Acta Cryst D. 2010; 66:213–221. [PubMed: 20124702]

Porcelli S, Brenner MB, Greenstein JL, Balk SP, Terhorst C, Bleicher PA. Recognition of cluster of differentiation 1 antigens by human CD4-CD8-cytolytic T lymphocytes. Nature. 1989; 341:447–450. [PubMed: 2477705]

Shamshiev A, Gober HJ, Donda A, Mazorra Z, Mori L, De Libero G. Presentation of the same glycolipid by different CD1 molecules. J Exp Med. 2002; 195:1013–1021. [PubMed: 11956292]

Spada FM, Grant EP, Peters PJ, Sugita M, Melian A, Leslie DS, Lee HK, van Donselaar E, Hanson DA, Krensky AM, et al. Self-recognition of CD1 by gamma/delta T cells: implications for innate immunity. J Exp Med. 2000; 191:937–948. [PubMed: 10727456]

Sugita M, van Der Wel N, Rogers RA, Peters PJ, Brenner MB. CD1c molecules broadly survey the endocytic system. Proc Natl Acad Sci U S A. 2000; 97:8445–8450. [PubMed: 10890914]

Sullivan BA, Kronenberg M. TCR-mediated recognition of glycolipid CD1 complexes. Curr Top Microbiol Immunol. 2007; 314:165–193. [PubMed: 17593661]

Summeren RPV, Moody DB, Feringa BL, Minnaard AJ. J Am Chem Soc. 2006; 128:4546–4547. [PubMed: 16594671]

Ulrichs T, Moody DB, Grant E, Kaufmann SH, Porcelli SA. T-cell responses to CD1-presented lipid antigens in humans with Mycobacterium tuberculosis infection. Infect Immun. 2003; 71:3076–3087. [PubMed: 12761085]

Van Rhijn I, Young DC, De Jong A, Vazquez J, Cheng TY, Talekar R, Barral DC, Leon L, Brenner MB, Katz JT, et al. CD1c bypasses lysosomes to present a lipopeptide antigen with 12 amino acids. J Exp Med. 2009; 206:1409–1422. [PubMed: 19468063]

Veronese FD, Copeland TD, Oroszlan S, Gallo RC, Sarngadharan MG. Biochemical and immunological analysis of human immunodeficiency virus gag gene products p17 and p24. J Virol. 1988; 62:795–801. [PubMed: 3123712]

Willcox BE, Willcox CR, Dover LG, Besra G. Structures and functions of microbial lipid antigens presented by CD1. Curr Top Microbiol Immunol. 2007; 314:73–110. [PubMed: 17593658]

Wu D, Zajonc DM, Fujio M, Sullivan BA, Kinjo Y, Kronenberg M, Wilson IA, Wong CH. Design of natural killer T cell activators: structure and function of a microbial glycosphingolipid bound to mouse CD1d. Proc Natl Acad Sci U S A. 2006; 103:3972–3977. [PubMed: 16537470]

Zajonc DM, Cantu C 3rd, Mattner J, Zhou D, Savage PB, Bendelac A, Wilson IA, Teyton L. Structure and function of a potent agonist for the semi-invariant natural killer T cell receptor. Nat Immunol. 2005a; 6:810–818. [PubMed: 16007091]

Zajonc DM, Crispin MD, Bowden TA, Young DC, Cheng TY, Hu J, Costello CE, Rudd PM, Dwek RA, Miller MJ, et al. Molecular mechanism of lipopeptide presentation by CD1a. Immunity. 2005b; 22:209–219. [PubMed: 15723809]

Zajonc DM, Elsliger MA, Teyton L, Wilson IA. Crystal structure of CD1a in complex with a sulfatide self antigen at a resolution of 2.15 A. Nat Immunol. 2003; 4:808–815. [PubMed: 12833155]

Zajonc DM, Maricic I, Wu D, Halder R, Roy K, Wong CH, Kumar V, Wilson IA. Structural basis for CD1d presentation of a sulfatide derived from myelin and its implications for autoimmunity. J Exp Med. 2005c; 202:1517–1526. [PubMed: 16314439]

Zajonc DM, Savage PB, Bendelac A, Wilson IA, Teyton L. Crystal structures of mouse CD1d-iGb3 complex and its cognate Valpha14 T cell receptor suggest a model for dual recognition of foreign and self glycolipids. J Mol Biol. 2008; 377:1104–1116. [PubMed: 18295796]

Zeng Z, Castano AR, Segelke BW, Stura EA, Peterson PA, Wilson IA. Crystal structure of mouse CD1: An MHC-like fold with a large hydrophobic binding groove. Science. 1997; 277:339–345. [PubMed: 9219685]

Zhou D, Cantu C 3rd, Sagiv Y, Schrantz N, Kulkarni AB, Qi X, Mahuran DJ, Morales CR, Grabowski GA, Benlagha K, et al. Editing of CD1d-bound lipid antigens by endosomal lipid transfer proteins. Science. 2004; 303:523–527. [PubMed: 14684827]

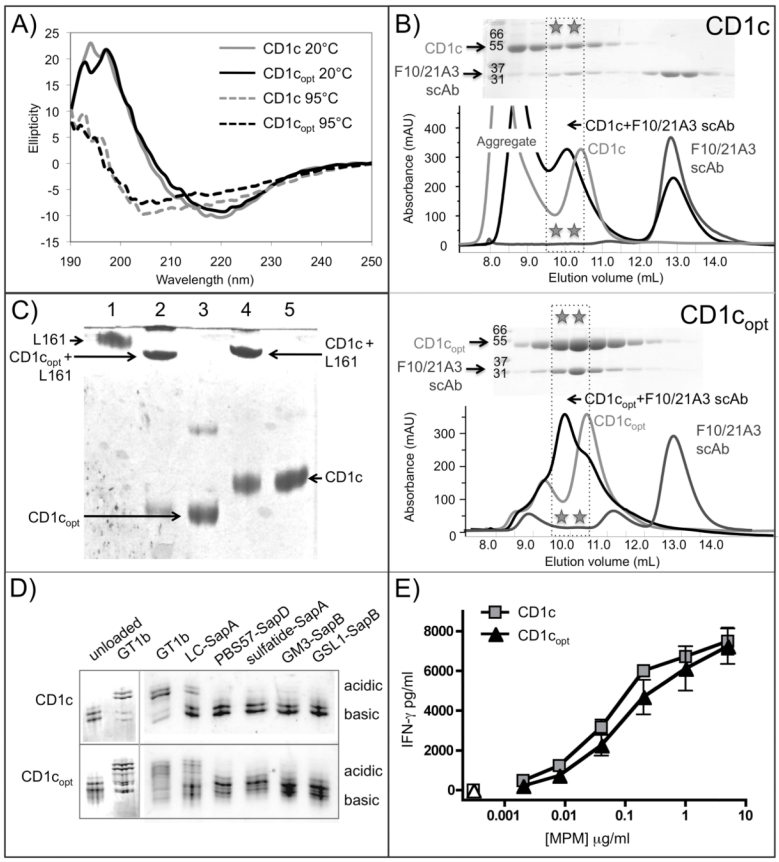

Figure 1. The α1 and α2 platform domains of CD1c and optimized CD1c (CD1copt) are structurally and functionally conserved

(A) CD spectra of CD1c and CD1copt at 20°C and 95°C. (B) The CD1c and CD1copt constructs both bind the F10/21A3 single-chain antibody as assessed by size exclusion chromatography. SDS-PAGE analysis of the shifted peak fractions confirms the presence of complexes between both CD1c and CD1copt with F10/21A3. (C) Both CD1c and CD1copt bind to the CD1c specific monoclonal antibody L161 (lanes 2 and 4, respectively) as evidenced by native gel shift compared to L161, CD1c or CD1copt alone (lanes 1, 3 and 5, respectively). (D) Loading efficiency of a variety of lipids is conserved between CD1c and CD1copt: CD1c or a fully glycosylated version of CD1copt are shown on a native isoelectric focusing gels as unloaded or loaded with the charged lipid GT1b (left box). Addition of saposins and a series of lipids resulted in similar shifting of the CD1c-GT1b and CD1copt-GT1b complexes upon displacement of GT1b (right box). Shown are: lactosylceramide (LC), PBS57, sulfatide, GM3 or GSL-1 and the indicated saposin. (E) CD1c-restricted T cell recognition of wild- type and optimized CD1c molecules. Wild-type and CD1copt proteins were coated on a micro-titer plate and pulsed with the indicated concentrations of synthetic MPM lipid (filled symbols), then washed and used to stimulate IFN-γrelease by the CD8–1 T cell line. Open symbols show CD8–1 T cell responses to wild-type and CD1copt molecules that were pulsed with vehicle alone. Shown are the means and standard deviations of IFN-γconcentrations from 3 replicates, as quantified by a standardized ELISA.

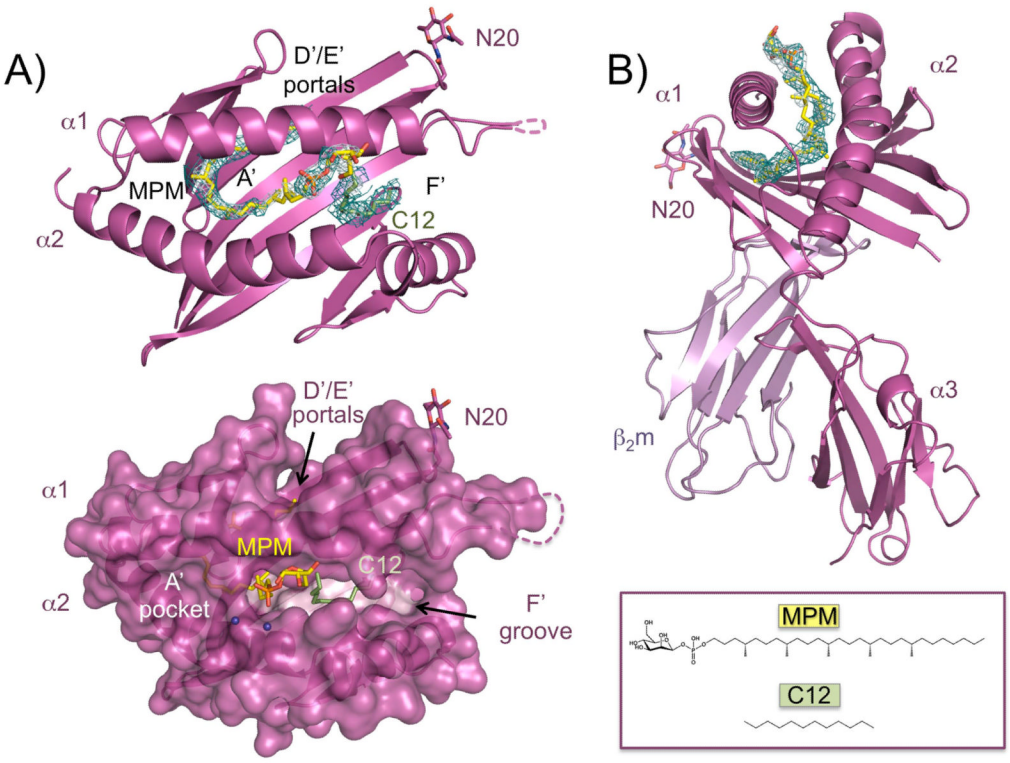

Figure 2. Structure of CD1c in complex with MPM and a C_{12} spacer lipid

(A) Top view of the ligand binding domain as a ribbon (top panel) and surface diagram (bottom panel). The CD1c heavy chain is shown in light magenta, MPM in yellow and C_{12} in light green. MPM is bound in the A′ pocket while a C_{12} is bound in the open F′ groove. Two ordered water molecules that solvate the MPM head group are shown as purple spheres. Omit map (green) and 2Fo-Fc (white) densities at a σ=1 and 1.4, respectively are shown for both ligands. (B) Side view of CD1c shown as a ribbon diagram with β_2m colored light purple. The alkyl chain of MPM is buried underneath the α1 helix, with its phosphomannose head group reaching out of the ligand-binding groove, accessible for recognition by a TCR. The chemical structures of MPM and C_{12} are shown in the bottom panel.

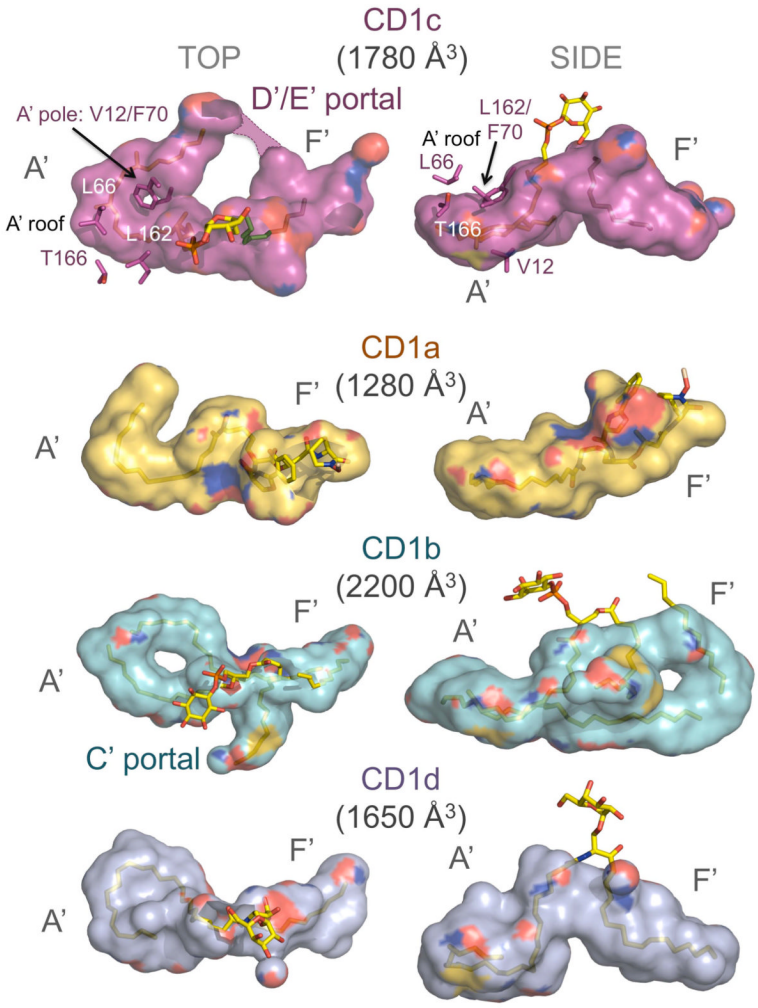

Figure 3. Comparison of antigen-binding cavities of human CD1 isoforms in complex with ligands

Top and side views of the binding cavities of CD1c (light magenta) with MPM and C_{12}, CD1a (yellow) with mycobactin (1XZ0), CD1b (cyan) with GM2 and spacer lipids (1GZQ) and CD1d (light purple) with α-galactosylceramide (1ZT4), shown as surface cavity representations. Red, blue and yellow surface colors represent the contribution of oxygen, nitrogen and sulfur atoms to the surface cavity, whereas ligands are colored with the following atom designations: carbon=yellow, oxygen=red, nitrogen=blue, and phosphorus=orange. Residues forming conserved features in CD1c are shown as sticks and colored as described above. Cavity volumes for each CD1 isoform were calculated with Pocket Finder(Hendlich et al., 1997) and are indicated in $Å^3$.

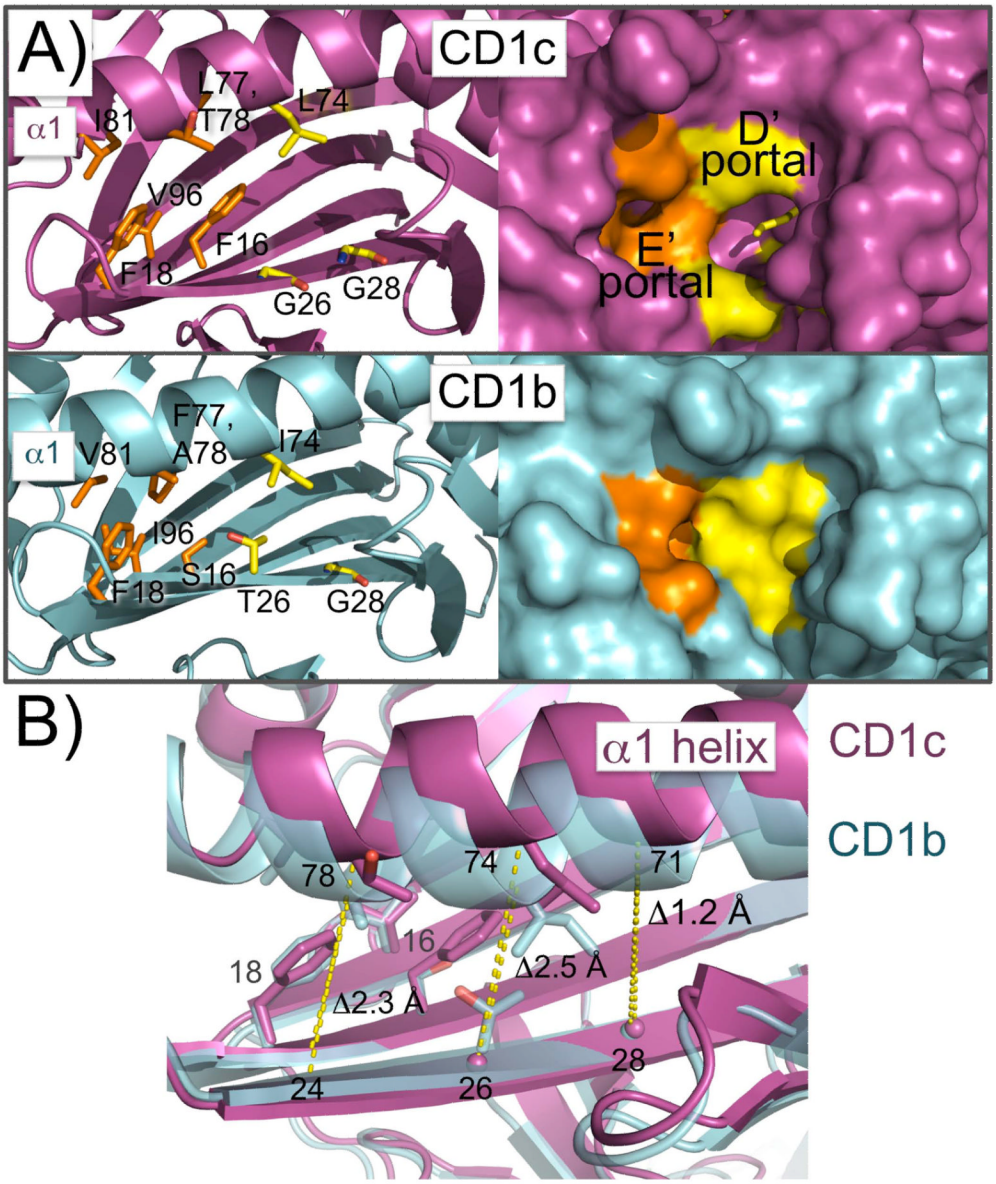

Figure 4. Unique features in CD1c: D′ and E′ portals

(A) Ribbon (left panel) and surface diagram (right panel) of the D′ and E′ portals in CD1c (magenta) and their comparison to CD1b (cyan). Residues forming the D′ and E′ portals in CD1c and corresponding residues in CD1b are shown in yellow and orange, respectively. (B) Overlay of ribbon diagrams of CD1c and CD1b reveal an increased distance between the α1 helix and the S1 strand of the α2 β-sheet in CD1c. The distances are shown as yellow dashes and the increase is indicated at three positions corresponding to the location of the D′ and E′ portals in CD1c.

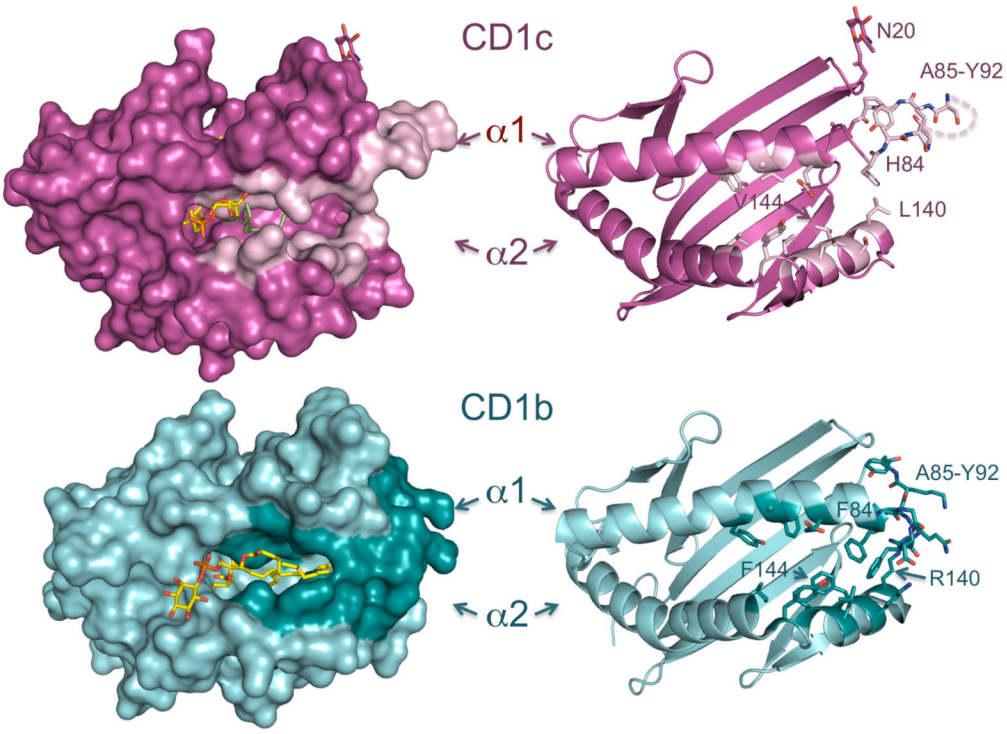

Figure 5. Residues and features forming the F′ groove in CD1c, and comparison to CD1b

Top view of a surface representation (left panel) and ribbon diagram (right panel) of CD1c (magenta, top panel) and CD1b (cyan, bottom panel). Residues lining the F′ groove in CD1c are shown in light pink and the corresponding residues in CD1b are shown in teal. The unresolved residues in the flexible loop connecting the CD1c α1 helix to the β-sheet are shown as a dashed line.

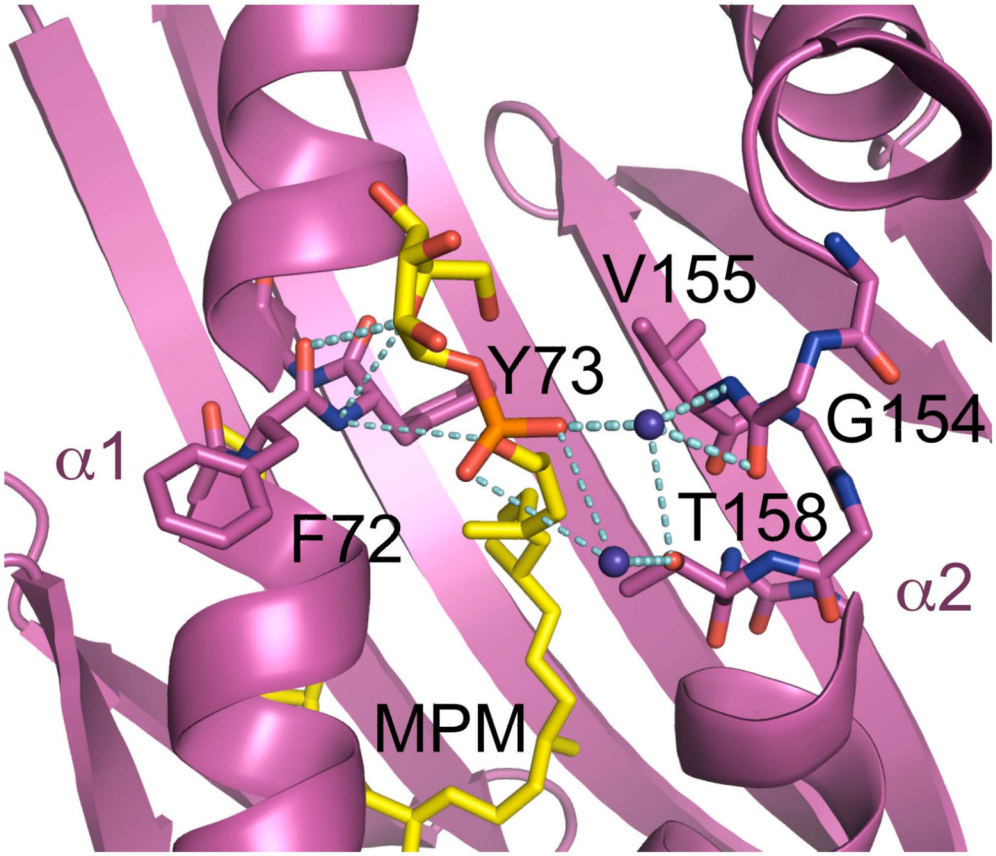

Figure 6. Hydrogen bonding network between CD1c and MPM

CD1c is shown as a ribbon diagram with residues involved in hydrogen bonding with MPM shown as sticks and labeled. Atoms are colored as such: yellow, carbon; blue, nitrogen; red, oxygen; orange, phosphorus. Two bound water molecules are shown as purple spheres. Highly probable hydrogen bonds are displayed as large dashes, potential ones as small dashes.

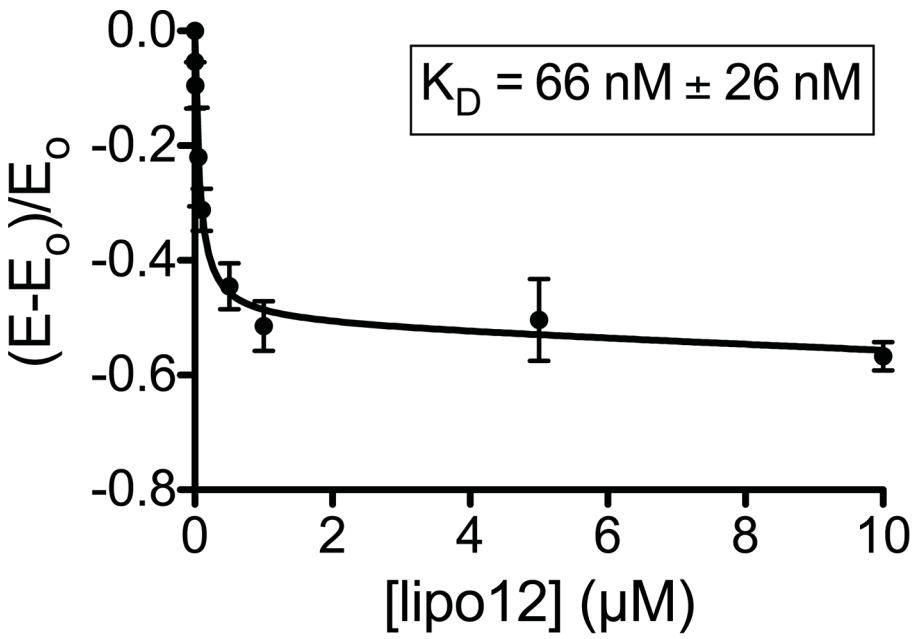

Figure 7. Analysis of lipopeptide binding to CD1c with fluorescence spectroscopy

A fixed concentration of CD1c was incubated with increasing concentrations of lipo-12 and the tryptophan fluorescence signal of the samples was measured. The quenching of tryptophan fluorescence with increasing amounts of lipo-12 was expressed as a ratio $(E-E_o)/E_o$, the change in fluorescence divided by the control fluorescence in the absence of added lipo-12. The data were fit to a one-site binding model to determine the apparent K_D of this interaction.

Table 1

Data collection and refinement statistics (molecular replacement)

Data collection	
Space group	$P2_12_12_1$
Cell dimensions	
a, *b*, *c* (Å)	53.72, 87.09, 88.81
αβγ(°)	90, 90, 90
Resolution (Å)	43.5–2.5 (2.54–2.50)*
R_{merge}	8.2 (52.1)
$I / \sigma I$	19.5 (1.9)
Completeness (%)	96.1 (76.6)
Redundancy	5.4 (2.3)
Refinement	
Resolution (Å)	43.5–2.5
No. reflections	14,397
R_{work} / R_{free}	24.0/27.3
No. atoms	
Protein	3,014
Lipid ligands	60
Water	38
B–factors	
Protein	55.7
Ligand/ion	53.7
Water	49.6
R.m.s. deviations	
Bond lengths (Å)	0.011
Bond angles (°)	1.490

Values in parentheses are for highest-resolution shell.